

FAST SDM FOR SHAPED REFLECTOR ANTENNA SYNTHESIS VIA PATCH DECOMPOSITIONS IN PO INTEGRALS

H.-H. Chou

Department of Engineering
Cambridge University
Cambridge CB3 0FA, U.K.

H.-T. Chou

Department of Communications Engineering
Yuan Ze University
Chung-Li 320, Taiwan

Abstract—This paper presents an approach of a shaped reflector antenna synthesis using a steepest decent method (SDM). It first discretizes the reflector surface into small patches and then uses grid nodes as variables in the synthesis procedure. Even though the number of variables can be very large for a large reflector antenna, the advantage of providing closed-form solutions for the derivatives of a cost function potentially makes this approach very efficient. The large number of variables also assists this procedure to reach a more global optimum as usually met in ordinary SDM. Numerical examples are presented to validate this approach.

1. INTRODUCTION

Fast design of large shaped reflector antennas remains challenging due to their increasing sizes needed in the applications of satellite and wireless communications [1–12]. Such challenges arise from the computational inefficiency in numerical radiation analysis that becomes dramatically cumbersome as the reflector size or operational frequency increase and needs to be repeatedly performed at every loop of an iterative synthesis procedure. In the past, efforts have been

Corresponding author: H.-H. Chou (hsihsirchou@gmail.com).

focused on developing fast radiation analysis or convergent synthesis techniques in a relatively independent fashion.

Typical works for the fast analysis techniques are presented in [13, 14], mostly using the approximations of physical optics (PO) or aperture integration (AI) by numerically integrating radiation integrals. These techniques are most widely employed in the reflector antenna analysis for practical applications. Either Fast Fourier Transform (FFT) or expansions over the integrands using properly selected bases, such as Gaussian beams (GB) [4, 5, 15], are performed with enduring sacrifice of accuracy. Previously, successfully employed synthesis techniques are referenced in [3, 8–12, 16–18] including genetic algorithm (GA) [11], steepest decent method (SDM) [3, 5, 8, 9], successive projection method (SPM) [10–12, 17] and particle swarm optimization (PSO) [18]. Acceleration efforts were attempted in two categories. The first tries to use fewer variables by representing reflector surfaces in terms of basis functions [7, 19, 20] and uses the associated coefficients as variables for optimization. It may however lose freedoms for global optimization. More reduction in the number of variables causes more freedom loss, and tradeoffs between efficiency and optimum must be made. The second attempts to develop analytic formulations for use in the optimization procedure [8–12]. In [8, 9], direct surface variations are considered, and analytical formulations for surface deviations based on the gradients of the cost function defined in a frame work of SDM were developed. It avoids numerical computations on the derivatives of a cost function, but still results in integrals that need to be numerically integrated using FFT. In [10–12] the reflector surface was discretized into patches. The radiations of each patch serve as basis functions to synthesize the desired contoured patterns, and SPM was employed to find coefficients of the basis functions using linear projections into the common intersection of available solution sets. The coefficients are transformed into the surface deviations by constraining an equal amplitude of the coefficients. It provides analytical and closed solutions for the surface variation. However, SPM does not guarantee the existence of the common intersected solutions, and the coefficients may be quite randomly distributed. In most cases, not only surface smooth techniques need to be performed in order to obtain continuous surface, but also rapid surface variation may occur.

This paper presents an useful technique of synthesis procedure. Analogous to that described in [8–12], it provides analytical formulations. Moreover, its formulations have advantages of being in closed forms and continuous for the reflector surface deviation. It completely avoids the numerical integrations and surface smoothing

required in [3, 8–12]. It first discretizes the reflector surface into small patches whose sizes are selected sufficiently small to accurately approximate the reflector's radiation by a superposition of each patch's component in the PO radiation integral. If the optimized surface is slowly varying, then the radiation analysis will retain the accuracy as usually provided by PO, which is found to be true in numerical experiences. The z -components of grid nodes' coordinates are used as variables in conjunction with a SDM synthesis technique to determine the shaped reflector surface. It looks, at a first glance, to complicate the synthesis procedure since the number of variables has now been increased dramatically to cause cumbersome numerical computations for the derivatives of a cost function in SDM. However, the proposed work using patch decompositions for the radiation integral exhibits advantages of providing approximate but in closed-form solutions for the derivatives. The overall computational efficiency is found to be improved.

The organization of this paper is as follows. Section 2.1 describes the formulations of patch decomposition to evaluate the PO radiation integral of a reflector antenna, which reduces the overall radiation in terms of a superposition of fields radiated from a set of equivalent current moments located at grid nodes. Section 2.2 summarizes SDM and presents the closed-form formulations for the derivatives of a cost function. Section 3 analyzes the computational complexity of this work, and presents numerical examples to validate the proposed work in the synthesis of a shaped reflector antenna. Finally some short discussions are presented in Section 4 to conclude this work. A time convention, $e^{j\omega t}$, is used throughout this paper.

2. THEORETICAL DEVELOPMENTS

2.1. Patches Decomposition of Physical Optics Radiation Integral

The radiation of a reflector antenna, when it is fed by (\bar{E}_f, \bar{H}_f) as illustrated in Figure 1, can be found by [9]

$$\bar{E}(\bar{r}) \cong \frac{jk}{4\pi} Z_0 \iint_S \hat{R} \times \hat{R} \times \bar{J}(\bar{r}') \frac{e^{-jkR}}{R} ds' \quad (1)$$

where $\bar{J}(\bar{r}') = 2\hat{n} \times \bar{H}_f(\bar{r}')$ is defined at \bar{r}' on S with \hat{n} being its an outward unit vector normal to the surface. $\bar{R} = \bar{r} - \bar{r}'$ with \bar{r} being a field location. Equation (1) can be numerically computed by

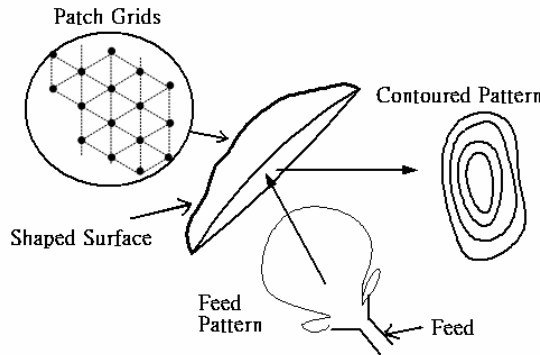


Figure 1. Geometry for the shaped reflector antenna problem in contoured beam application. The feed radiations (\bar{E}_f, \bar{H}_f) . The surface is decomposed into small planar pathes with grids also shown in this figure.

decomposing S into small patches and given by

$$\bar{E}(\bar{r}) \cong \sum_{m=1}^{N_m} \bar{E}_m(\bar{r}) \tag{2}$$

with

$$\bar{E}_m(\bar{r}) \cong \frac{jkZ_0}{4\pi} \frac{e^{-jkR_m}}{R_m} \hat{R}_m \times \hat{R}_m \times \iint_{\Delta S_m} \bar{J}(\bar{r}'_m) e^{jk\hat{R}_m \cdot \bar{r}'_m} ds' \tag{3}$$

where $S = \sum_{m=1}^{N_m} \Delta S_m$ with ΔS_m being the area of m th patch, $\bar{R}_m = \bar{r} - \bar{r}_{m0}$ and $\bar{r}'_m = \bar{r}' - \bar{r}_{m0}$ with \bar{r}_{m0} being the phase center of m th patch. N_m is selected that (2) will reach an acceptable accuracy as provided by PO. In general $\lambda/4$ patch width is sufficient in a practical case. As ΔS_m is sufficiently small and becomes approximately planar, (3) can be approximated by averaging their values at patch corners by

$$\bar{E}_m(\bar{r}) \cong \frac{jkZ_0}{4\pi} \frac{e^{-jkR_m}}{R_m} \Delta S_m \hat{R}_m \times \hat{R}_m \times \frac{1}{M_m} \sum_{p=1}^{M_m} \bar{J}_m(\bar{r}'_{mp}) e^{jk\hat{R}_m \cdot \bar{r}'_{mp}} \tag{4}$$

where \bar{r}'_{mp} indicates \bar{r}'_m at p th corner of m th patch, and M_m is the number of corners for m th patch. Thus in the far zone, (1) can be

re-expressed as a superposition of the contributions from corners by

$$\begin{aligned}\bar{E}(\bar{r}) &\cong \frac{jkZ_0}{4\pi} \frac{e^{-jkr}}{r} \hat{r} \times \hat{r} \times \sum_{q=1}^{N_c} e^{jk\hat{r}\cdot\bar{r}'_q} \sum_{m=1}^{N_q} \frac{\Delta S_m}{M_m} \bar{J}_m(\bar{r}'_q) \\ &= \frac{jkZ_0}{4\pi} \frac{e^{-jkr}}{r} \hat{r} \times \hat{r} \times \sum_{q=1}^{N_c} e^{jk\hat{r}\cdot\bar{r}'_q} \bar{I}_{eq,q}(\bar{r}'_q)\end{aligned}\quad (5)$$

where N_c is the number of corners formed by the patches and N_q is the number of patches associated with q th corner at \bar{r}'_q . The equivalent current moment, $\bar{I}_{eq,q}(\bar{r}'_q)$, in (5) is defined by

$$\bar{I}_{eq,q}(\bar{r}'_q) \equiv \sum_{m=1}^{N_q} \frac{\Delta S_m}{M_m} \bar{J}_m(\bar{r}'_q) = \Delta S_{eq,q} (2\hat{n}_{eq,q} \times \bar{H}_f(\bar{r}'_q)) \quad (6)$$

with

$$\Delta S_{eq,q} \hat{n}_{eq,q} = \sum_{m=1}^{N_q} \frac{\Delta S_m \hat{n}_m}{M_m}, \quad (7)$$

which is an equivalent surface vector associated with q th corner. In (6) and (7) $\bar{J}_m(\bar{r}'_q) = 2\hat{n}_m \times \bar{H}_f(\bar{r}'_q)$ with \hat{n}_m being \hat{n} at m th patch. Equation (5) is dependent on the corners' parameters, and allows one to employ the corner locations as the optimization variables. A practical implementation selects the locations of corners first, which globally distribute over the reflecting surface, and determine the patches.

2.2. Efficient Synthesis Procedure via Steepest Decent Method

SDM gives gradual parameters' changes in reflector surface variations, and results in a smooth reflector surface. It first defines a cost function in terms of sampled radiations patterns as [3]

$$\Phi = \sum_{\ell=1}^{N_s} f_\ell \left| G_\ell - G_\ell^d \right|^2 \quad (8)$$

where N_s is a number of samples and G_ℓ is the normalized gain at ℓ th field point with G_ℓ^d being its desired value. It will be minimized to optimize the reflector surface. Both sidelobe and cross-polarization levels are controlled by specifying G_ℓ^d in the sampled points, and are considered as different sampled gains. f_ℓ is introduced in (8) to

emphasize some desired gains, which is useful for side-lobe and cross-polarization suppression since their values are very small.

In SDM the variables, $\beta_q (q = 1 \sim Q)$ with Q being the number of variables to define the reflector surface, is optimally changed in an iterative fashion using (9), that is, β_q at $(i + 1)$ th iteration is found by [6]

$$\begin{bmatrix} \beta_1 (i + 1) \\ \beta_2 (i + 1) \\ \vdots \\ \beta_Q (i + 1) \end{bmatrix} = \begin{bmatrix} \beta_1 (i) \\ \beta_2 (i) \\ \vdots \\ \beta_Q (i) \end{bmatrix} - \mu \begin{bmatrix} \frac{\partial \Phi}{\partial \beta_1} \Big|_{\beta_1 = \beta_1(i)} \\ \frac{\partial \Phi}{\partial \beta_2} \Big|_{\beta_2 = \beta_2(i)} \\ \vdots \\ \frac{\partial \Phi}{\partial \beta_Q} \Big|_{\beta_Q = \beta_Q(i)} \end{bmatrix} \tag{9}$$

where μ is a scale factor to proper minimize (8). The implementation procedure is demonstrated in Figure 2.

Numerical computations of the derivatives in (9) are cumbersome because as β_q changes, indicating a new surface shape of reflector, (1) needs to be re-calculated, which increases dramatically as Q increases. In the past, the value of Q needs to be first minimized by expanding the surface using either global or local basis functions such as Jacobi-Fourier series [7] and spline [14], respectively. Two disadvantages are found. First, repeatedly computations of (1) are extremely cumbersome since β_q changes frequently during SDM. Secondly, a small Q limits the freedom of surface variation. This work, employing coners

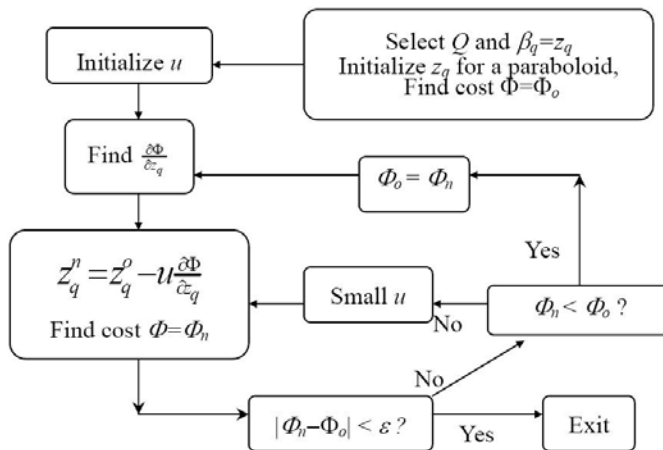


Figure 2. SDM synthesis procedure.

of the patched as optimization variables, allows a maximum freedom in varying the surface for a global optimization. The surface shape is determined by corner locations. In particular, z_q of the q th corner's coordinate, $\vec{r}'_q = (x_q, y_q, z_q)$, are used as variables (i.e., $\beta_q = z_q$) while fixing (x_q, y_q) to retain the projected aperture of the reflector.

At a first glance, this work increase Q up to several orders and may worsen the optimization. It however exhibits advantages of providing closed-form solutions for the derivatives in (9) because each corner, (x_q, y_q, z_q) , is associated with very few patches as illustrated in Figure 1. The derivative in (9) can be found by differentiating (8)

$$\frac{\partial \Phi}{\partial z_q} = 2 \sum_{\ell=1}^{N_s} \left[f_\ell \frac{\partial G_\ell}{\partial z_q} (G_\ell^- G_\ell^d) \right] \tag{10}$$

where

$$\frac{\partial G_\ell}{\partial z_q} = \frac{8\pi}{Z_0 P_r} \text{Re} \left[(\vec{E}(\vec{r}_\ell) \cdot \hat{v}_\ell) \left(\frac{\partial \vec{E}(\vec{r}_\ell)}{\partial z_q} \cdot \hat{v}_\ell \right) \right] \tag{11}$$

and using (5) gives

$$\frac{\partial \vec{E}(\vec{r})}{\partial z_q} \cong \frac{k^2 Z_0 (b_3 - a_3)}{4\pi} \frac{e^{-jkr} e^{jk\hat{r} \cdot \vec{r}'_q}}{r} \hat{r} \times \hat{r} \times \vec{I}_{eq,q}(\vec{r}'_q). \tag{12}$$

In (11), P_r is the radiation power, $\hat{r} = (a_1, a_2, a_3)$ and $\frac{\vec{r}'_q - \vec{r}_f}{|\vec{r}'_q - \vec{r}_f|} = (b_1, b_2, b_3)$ with \vec{r}_f being the feed's location. \hat{v}_ℓ is the unit vector indicating the polarization of interest, and may be used to specify co- or cross-polarizations. Note that (10) is a closed-form solution, and is continuous over the surface. Not only the derivatives of (8) can be efficiently computed, but also the synthesized surface retains smooth along the iterative procedure. Once the corner locations are determined and fixed, the surfaces between these corners can be interpolated and smooth using local basis functions such as these described in [19, 20] without losing the accuracy of the radiation patterns. As a result, if the distributions of the corners are shown to be continuous and smooth, then the smoothness of the overall surface can be assured.

2.3. A Useful Criterion to Choose μ

SDM uses (9) to update z_q iteratively. The changes of z_q , Δz_q , in each iteration are controlled by a proper selection of μ , and result in phase changes for the equivalent moments in (6) in a way that the superposition of their radiations will approach the desired contoured

patterns. It can be achieved by allowing Δz_q varying within a half wavelength. The value of μ is selected such that maximum Δz_q in each iteration is less than a half wavelength. A good value is less than 0.25 wavelength that represents a maximum phase change of 180 degrees ($-0.25\lambda \sim 0.25\lambda$ causes a maximum phase change of 180 degrees) so that the overall maximum Δz_q after the completion of synthesis may retain less than a half wavelength. In practice, μ should be continuously decreases as the synthesis proceeds since SDM converges very fast in the first few rounds of iteration and Δz_q will become gradually smaller. One may simply decrease μ to a quarter or 0.1 of its value in the previous iteration when the value of cost function in (8) is found to increase, and retain this value for the next iteration.

2.4. Advantages and Limitations of the Proposed Work

In comparison with previous SDM works [3, 5, 8, 9], the current approach exhibits advantages. In [3], the grids of the equivalent aperture based on AI are used as optimization variables. It requires performing ray-tracing to determine the reflector's surface which needs to be smoothed to retain a continuous surface. The proposed work completing avoids these. In [5], a reflector surface is represented by a set of global basis functions to reduce the number of optimization variables and computational time. The proposed work uses surface grids as optimization variables. It has a much larger number of optimization variables, but results in less computational time as to be shown in Section 3. In comparison with [8, 9], which also provides closed form solutions, the proposed work doesn't require performing FFT in computing the solution. The limitations of the proposed work can be observed. First, the number of optimization variables increases in an order of reflectors surface size. Second, the increase will further increase the size of computer's memory. These limitation do not cause any inconvenience in practical applications with today's computer technologies in hand.

3. NUMERICAL VALIDATION AND DISCUSSION

3.1. Analysis of Computational Complexity

The computational complexity, justified by counting the number of terms the operation of summations in each iteration of numerical evaluation, is examined. One first examines the computation complexity in a traditional SDM [5]. Assuming that N_b basis functions are used to represent the reflector surface in a conventional SDM, the number of terms is counted in the following. Using (5) to find the

electromagnetic fields at N_s points for (8) requires $N_c \times N_s$ terms. In each iteration one needs to find $N_b(Q = N_b$ in (9)) derivatives numerically for (9), and it requires $N_c \times N_s \times N_b$ terms. Similarly the number of terms in the proposed work is counted in the following. Using (5) to find the the electromagnetic field at N_s points for (8) needs $N_c \times N_s$ terms. Using (9) to find N_m derivatives ($N_m \leq N_c$) for (9) needs to compute $N_m \times N_s$ terms. Therefore if the number of iterations is not considered, the proposed work apparently has a better efficiency by cutting the computational complexity in an order of N_b .

3.2. Numerical Examples

The example shown in [3] is re-examined to produce a CONUS beam with power constraints within 3 dB. The initial surface is parabolic with a focal length 25λ . The radius of a projected circular aperture on the x - y plane is 12.5λ , with an offset distance 3λ to avoid a feed blockage. The operational frequency is 11.811 GHz. The feed has a $\cos^{11.25} \theta$ radiation pattern with a right hand circular polarization. This initial reflector surface will radiate far fields with a directivity of 38.0 dB with roughly 5 square degrees beam area. To achieve the beam constraints shown in Figure 3, the maximum directivity is roughly 30 dB. Thus the desired goal of directivity in the specified area of Figure 3 will be larger than 28 dB, where f_i in (8) is set to one for simplification. The maximum deviation, Δz_q , is initially set to be 0.2 wavelength, which is gradually decreased by a factor of 0.25 when the cost function is found to increase in the iterative procedure.

In a practical implementation, the surface change at first iteration represents the steepest surface variations to minimize the cost function by defocusing the focused fields radiated from a parabolic reflector. This rapid surface change for energy defocusing may eventually results

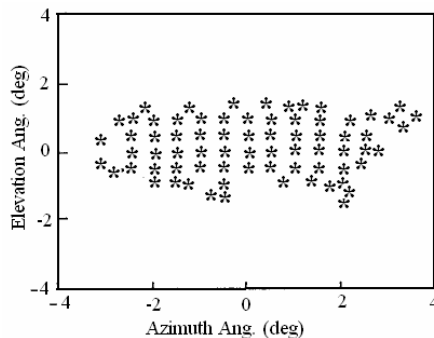


Figure 3. Desired CONUS contoured pattern.

in a rapid surface variation that is not considered to be sufficient smooth from a point of view in a realistic manufacture. Figure 4(a) shows the derivatives of the cost function using (11), which is normalized in a way that the vector formed by these derivatives has a unit norm and represents the changing rate of Δz_q . Also Figure 5(a) shows the contoured radiation patterns after this surface change. Note that the maximum change length of Δz_q is restricted to 0.2λ in this case as mentioned in the previous paragraph. In particular, Figure 4(a) shows that the surface distorts with a variation similar to a sine function. It tends to spread the energy out in upward and downward directions as shown in Figure 5(a), where two beams were formed in the

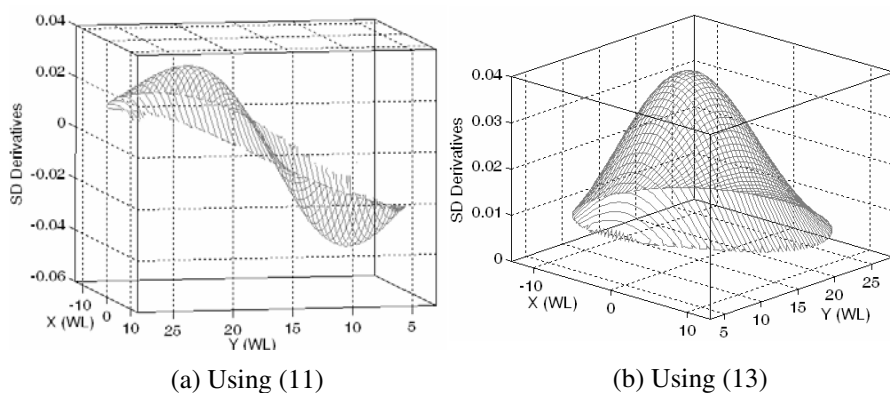


Figure 4. Comparison of initial derivatives of the cost function used in SDM.

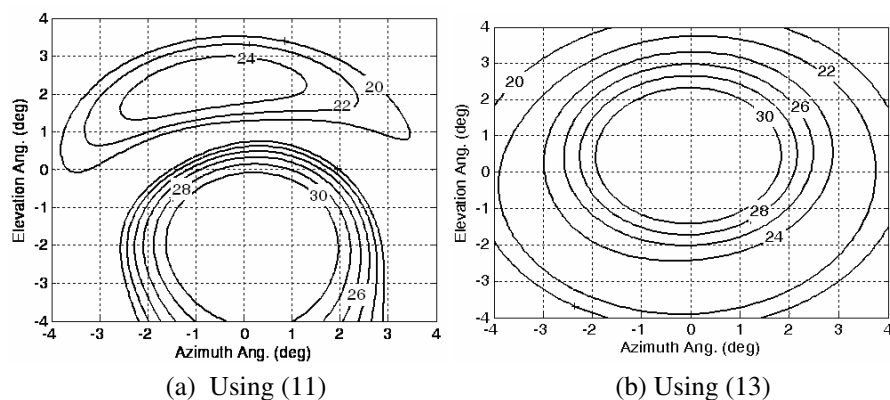


Figure 5. Contoured radiation patterns at first iteration.

coverage area. To avoid this phenomenon, an alternative formulation is used at first iteration. The idea is to consider the behavior of the power derivatives used in (11), where a real part is used and exhibits a sine function behavior. Thus it can be conjectured that its imaginary part will have a cosine function behavior. Figure 4(b) shows the surface changing rate corresponding to Figure 4(a) except now (11) is replaced by

$$\frac{\partial G_\ell}{\partial z_q} = -\frac{8\pi}{Z_0 P_r} \text{Im} \left[(\bar{E}(\bar{r}_\ell) \cdot \hat{v}_\ell) \left(\frac{\partial \bar{E}(\bar{r}_\ell)}{\partial z_q} \cdot \hat{v}_\ell \right) * \right], \quad (13)$$

where “-” sign is employed to assure positive surface variations for convenience. The corresponding radiation pattern at first iteration is shown in Figure 5(b). It is observed that the energy spreads out concentrically. This gradual energy distribution allows the synthesis to reach a better smoothness for its use in manufacture. Afterward, (11) is employed to synthesize the surface. To further examine the smoothness of the reflector, Δz_q changing rates at 2nd, 7th and 21th iterations are shown in Figures 6(a)~(c), respectively. First, Figure 6(a) shows that the behavior of Δz_q changing rate is similar to that in Figure 4(b). It indicates that SDM continues to defocus the radiating energy after its initial iteration. Once the energy defocusing has sufficiently cover the desired area, SDM starts to modify the surface such that the radiation will form the shaped pattern as shown in Figures 6(b) and (c). Note that the maximum of Δz_q changing length decreases along the synthesis procedure. Figure 7(a) shows the changes of maximum Δz_q during the synthesis procedure, which makes the cost function continuously decreases. The decreases on Δz_q is necessary in order to avoid wasting time in computing the values of cost function which tends to increase along the synthesis procedure if the maximum Δz_q is retained same in each iteration. Also Figure 7(b) shows the convergence of the cost function along the synthesis. The cost function converges very fast in the first few rounds of iteration and the rate slows down after 50 iterations. Thus after 50 iterations, the slow convergence rate will result in smaller changes in the cost function and surface variations of the reflector as well, which justifies the need to use a smaller μ . This is advantageous over other techniques where global or local basis functions are used to represent the reflector surface since no prior knowledge on the selection of μ appears. In the current example, only 60 iterations are performed to achieve the contoured patterns shown in Figure 8(a), where 73 sampled field points are considered. The maximum directivity is 30.5 dB in this case. The computation of (5) uses triangular patches with a 0.25 wavelength sampling length, which is sufficient to compute the fields located in the angular area of interest ($\theta < 4^\circ$), and results in 8154 corners (also 8154 variables) in

the synthesis procedure. This number of variables is far larger than the number of field points to be synthesized. Thus it reduces the possibility of cost function's convergences stuck in a local minimum before a reasonable result is achieved.

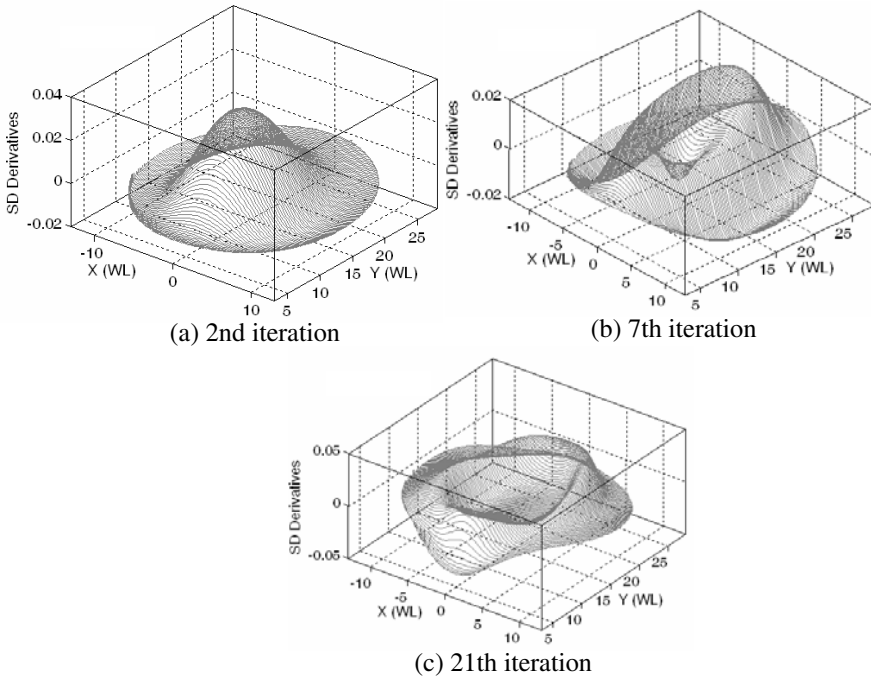


Figure 6. Derivatives of the cost function with respect to the optimization variables using (11).

The computational efficiency can be further improved. Note that (5) is simply used to compute the radiation fields, which can be further accelerated if other efficient techniques are available such as the analysis techniques based on a Gaussian beam expansion [4, 5, 10]. The deviation of the shaped surface from the original (initial) parabolic reflector is also shown in Figure 8(b) for comparison. As described earlier that the derivatives of the cost function with respect to Δz_q are continuous, which assures the continuity and smoothness of the synthesized surface as demonstrated in Figure 8(b) where smooth surface deviation is observed.

Finally the CPU time, running on an Acer Notebook with Intel 2.2 GHz Core 2 Duo Processor T7500, is 0.28 seconds for the computation in an iteration with total time less than 20 second to

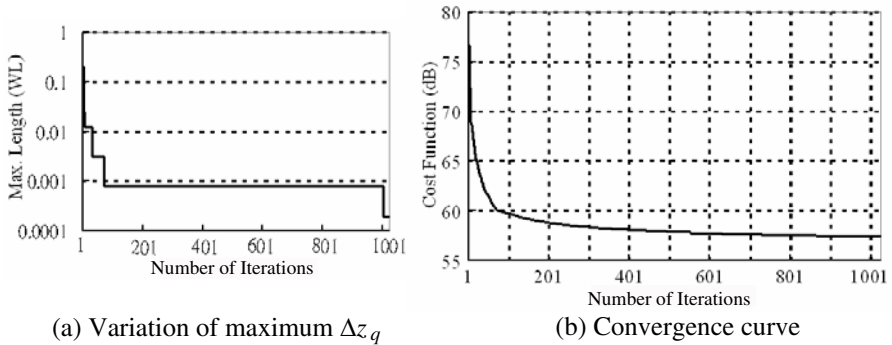


Figure 7. Changes of maximum Δz_q and the convergence curve along the synthesis procedure.

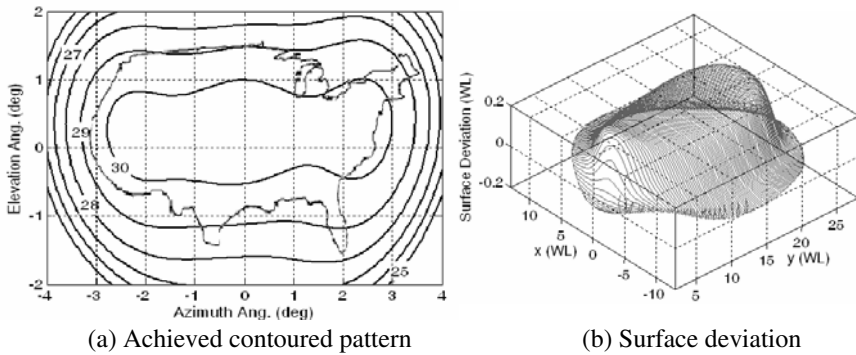


Figure 8. The achieved contoured pattern and the surface deviation (unit: wavelength) after the complete of synthesis.

complete 60 iterations of synthesis and achieve the results shown in Figure 8(a).

4. CONCLUSION

This proposed work is very effective in the fast synthesis of shaped reflector antennas to radiate contoured beams. This method exhibits largest freedoms by using a large number of variables in the synthesis, where the surface grid nodes are used. Closed form and continuous solutions of cost function's derivatives are developed, which allows the surface varying smoothly while, in the mean time, retaining the computational efficiency. Numerical examples show that the

computational complexity in this work can be reduced by an order of Q (the number of variables in the traditional SDM using numerical computations to find the derivatives of a cost function).

ACKNOWLEDGMENT

Financial support for this work from the National Science Council, Taiwan, is acknowledged.

REFERENCES

1. Rudge, A. W., K. Milne, A. D. Olver, and P. Knight, *The Handbook of Antenna Design*, Vol. 1, Peter Peregrinus, London, 1982.
2. Rusch, W. V. T., "The current state of the reflector antenna art," *IEEE Trans. Antennas Propagat.*, Vol. 32, 313–329, 1984.
3. Cherrette, A. R., S. W. Lee, and R. J. Acosta, "A method for producing a shaped contour radiation pattern using a single reflector and a single feed," *IEEE Trans. Antennas Propagat.*, Vol. 37, No. 6, 698–702, Jun. 1989.
4. Chou, H. T., P. H. Pathak, and R. J. Burkholder, "Novel Gaussian beam method for the rapid analysis of large reflector antennas," *IEEE Trans. Antennas Propagat.*, Vol. 49, 880–893, Jun. 2001.
5. Chou, H.-T. and P. H. Pathak, "Fast gaussian beam based synthesis of shaped reflector antennas for contoured beam applications," *IET Proceeding-Microwave, Antenna and Propagations*, Vol. 151, No. 1, 13–20, Feb. 2004.
6. Theunissen, W., "Reconfigurable contoured beam synthesis using a mechanical fem surface description of dual offset reflector antenna surfaces," Ph.D. dissertation, University of Pretoria, South Africa, 1999.
7. Duan, D. and Y. R.-Samii, "A generalized diffraction synthesis technique for high performance reflector antennas," *IEEE Trans. Antennas Propagat.*, Vol. 43, 27–40, Jan. 1995.
8. Westcott, B. S. and A. A. Zaporozhets, "Single reflector synthesis using an analytical gradient approach," *Electronics Letters*, Vol. 30, No. 18, 1462–1463, Sep. 1, 1994.
9. Westcott, B. S. and A. A. Zaporozhets, "Dual-reflector synthesis based on analytical gradient-iteration procedures," *IET Proceeding-Microwave, Antenna and Propagations*, Vol. 142, No. 2, 129–135, Apr. 1995.

10. Poulton, G. T. and S. G. Hay, "Efficient design of shaped reflectors using successive projections," *Electronics Letters*, Vol. 27, 2156–2158, 1991.
11. Hay, S. G., "Dual-shaped-reflector directivity pattern synthesis using the successive projections method," *IET Proceeding-Microwave, Antenna and Propagations*, Vol. 146, No. 2, 119–124, Apr. 1999.
12. Stirland, S. J., "Fast synthesis of shaped reflector antennas for contoured beams," *Proceedings of the ICAP 1993*, 18–21, Edinburgh, UK, 1993.
13. Bucci, O. M., A. Capozzoli, and G. D'Elia, "An effective power synthesis technique for shaped, double-reflector multifeed antennas," *Progress In Electromagnetics Research*, PIER 39, 93–123, 2003.
14. Pathak, P. H., "Techniques for high-frequency problems," *Antenna Handbook — Theory, Application and Design*, (by Y. T. Lo and S. W. Lee), Chapter 4, Van Nostrand Reinhold Company, New York, 1988.
15. Chou, H. T. and P. H. Pathak, "Uniform asymptotic solution for the em reflection and diffraction of an arbitrary gaussian beam by a smooth surface with an edge," *Radio Science*, 1319–1336, Jul.–Aug., 1997
16. Agastra, E., G. Bellaveglia, L. Lucci, R. Nesti, G. Pelosi, G. Ruggerini, and S. Selleri, "Genetic algorithm optimization of high-efficiency wide-band multimodal square horns for discrete lenses," *Progress In Electromagnetics Research*, PIER 83, 335–352, 2008.
17. Poulton, G. T., "Power pattern synthesis using the method of successive projections," *IEEE Antenna and Propagation Society International Symposium*, Vol. 2, 667–670, 1986.
18. Mikki, S. M. and A. A. Kishk, "Physical theory for particle swarm optimization," *Progress In Electromagnetics Research*, PIER 75, 171–207, 2007.
19. Pereira, L. and F. Hasselmann, "Approximation of shaped reflector surfaces by pseudo-splines," *IEEE Antennas and Propagation Society International Symposium*, Vol. 22, 327–329, Jun. 1984.
20. Teixeira, F. L., J. R. Bergmann, and C. Rego, "A comparison between techniques for global surface interpolation in shaped reflector analysis," *IEEE Trans. on Antennas Propagat.*, Vol. 42, No. 1, 47–53, Jan. 1994.